

Available online at www.sciencedirect.com

Virology 366 (2007) 349–360

VIROLOGYwww.elsevier.com/locate/yviro

Characterization of an antigenic site that contains a dominant, type-specific neutralization determinant on the envelope protein domain III (ED3) of dengue 2 virus

Gregory D. Gromowski, Alan D.T. Barrett *

Department of Pathology, Sealy Center for Vaccine Development, Center for Biodefense and Emerging Infectious Diseases, and Institute for Human Infections and Immunity, University of Texas Medical Branch, Galveston, TX 77555-0609, USA

Received 13 March 2007; returned to author for revision 22 March 2007; accepted 22 May 2007

Available online 23 August 2007

Abstract

The surface of the mature dengue virus (DENV) particle consists of 90 envelope (E) protein dimers that mediate both receptor binding and fusion. The E protein ectodomain can be divided into three structural domains designated ED1, ED2, and ED3, of which ED3 contains the critical and dominant virus-specific neutralization sites. In this study the ED3 epitopes recognized by seven, murine, IgG1 DENV-2 type-specific, monoclonal antibodies (MAbs) were determined using site-directed mutagenesis of a recombinant DENV-2 ED3 (rED3) protein. A total of 41 single amino acid substitutions were introduced into the rED3 at 30 different surface accessible residues. The affinity of each MAb with the mutant rED3s was assessed by indirect ELISA and the results indicate that all seven MAbs recognize overlapping epitopes with residues K305 and P384 critical for binding. These residues are conserved among DENV-2 strains and cluster together on the upper lateral face of ED3. A linear relationship was observed between relative occupancy of ED3 on the virion by MAb and neutralization of the majority of virus infectivity (~90%) for all seven MAbs. Depending on the MAb, it is predicted that between 10% and 50% relative occupancy of ED3 on the virion is necessary for virus neutralization and for all seven MAbs occupancy levels approaching saturation were required for 100% neutralization of virus infectivity. Overall, the conserved antigenic site recognized by all seven MAbs is likely to be a dominant DENV-2 type-specific, neutralization determinant.

© 2007 Elsevier Inc. All rights reserved.

Keywords: Dengue; Flavivirus; Envelope protein domain III; Neutralization; Monoclonal antibodies

Introduction

Dengue (DEN) is the most important mosquito-borne viral disease in terms of the number of cases each year and its geographic distribution. It is estimated that 2.5 billion people are at risk for DEN worldwide, with 50–100 million infections each year, including 250,000–500,000 cases of dengue hemorrhagic fever (DHF) (Halstead, 1988; Monath, 1994). DEN is a disease caused by four genetically and antigenically related viruses termed DENV-1, DENV-2, DENV-3, and DENV-4. There is extensive antigenic cross-reactivity between the DEN viruses but only limited, short-term, cross-protective immunity in humans (Sabin, 1952). Consequently, humans can have four separate DENV infections.

The DENV are members of the genus *Flavivirus*, family *Flaviviridae*, and have a positive-sense, single-stranded, RNA genome of approximately 11 kb in length (Chambers et al., 1990). They have a relatively simple enveloped virion that is 50 nm in diameter and consists of a capsid protein (C), membrane protein (M), and a major envelope glycoprotein (E) (Kuhn et al., 2002). The surface of the mature DENV virus particle consists of 90 E protein dimers (Kuhn et al., 2002; Zhang et al., 2003) that mediate both receptor binding (Crill and Roehrig, 2001) and fusion (Allison et al., 1995, 2001; Heinz and Allison, 2000).

The E protein is approximately 500 amino acids in length of which the N-terminal 400 amino acids form the ectodomain. The E protein ectodomain can be divided into three structural domains designated domain I, domain II, and domain III (ED1, ED2, and ED3, respectively) (Modis et al., 2003). ED1 is centrally located in the folded monomer, while ED2 is involved

* Corresponding author.

E-mail address: abarrett@utmb.edu (A.D.T. Barrett).

with dimerization of E protein monomers on the surface of the mature virion. ED2 also contains the fusion peptide, which is necessary for low-pH triggered fusion with the endosomal membrane and release of viral RNA into the cell cytoplasm (Allison et al., 2001). ED3 has an immunoglobulin-like fold, which is characteristic of many cell receptors. In addition, the flavivirus ED3 contains the critical and dominant virus-specific neutralization site(s) (Roehrig, 2003). In terms of the DENVs, ED3 elicits neutralizing antibodies that are predominantly DENV type-specific and are the most effective in terms of blocking virus adsorption to susceptible cells (Crill and Roehrig, 2001; Hung et al., 1999). Thus, ED3 has been implicated as the primary receptor-binding motif.

Compared to other flaviviruses, there has been relatively little work reported on fine mapping of neutralizing epitopes for DENV. DENV-2 neutralizing antibodies have been mapped to ED2, near the fusion loop, and ED3 (Roehrig et al., 1998). Some DENV neutralizing epitopes have been mapped to specific amino acids within ED3 by generating monoclonal antibody (MAb) resistant variants for DENV-2 (Hiramatsu et al., 1996; Lin et al., 1994; Lok et al., 2001) and DENV-3 (Serafin and Aaskov, 2001), but none for DENV-1 or DENV-4. Tirawatanapong et al. (1992) used overlapping peptides of ED3 to map the epitope of DENV-2 type-specific MAb 3H5 to amino acids 386–397 of the E protein. These results differed from those of Roehrig et al. (1990) who used similar peptides, derived from DENV-2 strain Jamaica 83, for epitope mapping and found that a peptide from amino acids 388–400 did not bind to MAb 3H5. Interestingly, the epitope mapped by Tirawatanapong et al. (1992) is adjacent, in the linear sequence of E, to the epitope mapped by Hiramatsu et al. (1996) (residues 383–385 of ED3) using mutagenesis of a DENV infectious clone. Peptides of ED3 have also been used to map a DENV complex MAb, 4E11, to a linear epitope consisting of residues 306–314 of the E protein (Thullier et al., 2001).

All of the above epitope mapping studies for DENV report linear epitopes or epitopes that consist of single amino acids.

However, structural studies of antibodies in complex with ED3s from two other flaviviruses, Japanese encephalitis virus (JEV) (Wu et al., 2003) and West Nile virus (WNV) (Kaufmann et al., 2006; Nybakken et al., 2005), revealed that there are several amino acid contacts at the binding interface between the antibody and ED3, and these amino acids form conformational epitopes. Thus, a more thorough analysis of DENV neutralizing epitopes will provide a better understanding of the molecular mechanism of DENV neutralization and aid in the development of candidate DENV vaccines.

In this study the epitopes recognized by seven DENV-2 type-specific MAbs were determined using site-directed mutagenesis of a recombinant DENV-2 ED3 (rED3) protein. The results indicate that all seven MAbs recognize a similar antigenic site that is conserved among DENV-2 strains and is located on the upper lateral face of ED3. Also, a comparison of plaque reduction neutralization (PRNT) curves and ELISA binding curves using whole DENV-2 virions as antigen indicates that there is a linear relationship between relative occupancy of this antigenic site on ED3 by MAb and neutralization of the majority of virus infectivity. These data will be valuable for the rationale design of a DENV-2 vaccine that elicits antibodies against this highly conserved antigenic site.

Results

Characterization of MAbs

All seven MAbs (3H5, M8051122, 9F16, 2Q1899, 1P-05-143, GTX77558, and 5C36) were shown to recognize the DENV-2 strain New Guinea C (NGC) rED3 by Western blotting (Fig. 1) and were shown to be specific for DENV-2 by indirect ELISA with rED3s from DENV-1 strain OBS7690, DENV-2 strain NGC, DENV-3 strain H87, and DENV-4 strain 703-4, with MBP used as a negative control (Fig. 2). The Kd of all seven MAbs was determined for the DENV-2 NGC rED3 by titration in an indirect ELISA, as described in Materials and

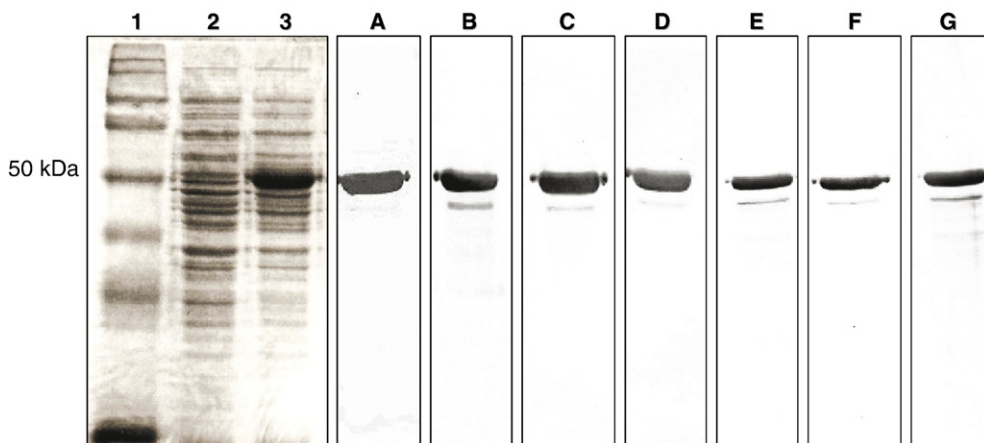


Fig. 1. Western blot of anti-DENV-2 monoclonal antibodies. The non-reducing protein gel, shown in lanes 1, 2, and 3, was stained with brilliant blue and in each of the lanes are (1) rainbow marker, (2) “uninduced” bacterial extract, and (3) “induced” DENV-2 MBP-rED3 bacterial extract. Lanes A to G are non-reducing Western blots showing recognition of the DENV-2 MBP-rED3 by MAbs (A) 3H5, (B) M8051122, (C) 9F16, (D) 2Q1899, (E) 1P-05-143, (F) GTX77558, and (G) 5C36. All seven MAbs recognize the approximately 50 kDa DENV-2 MBP-rED3 fusion protein.

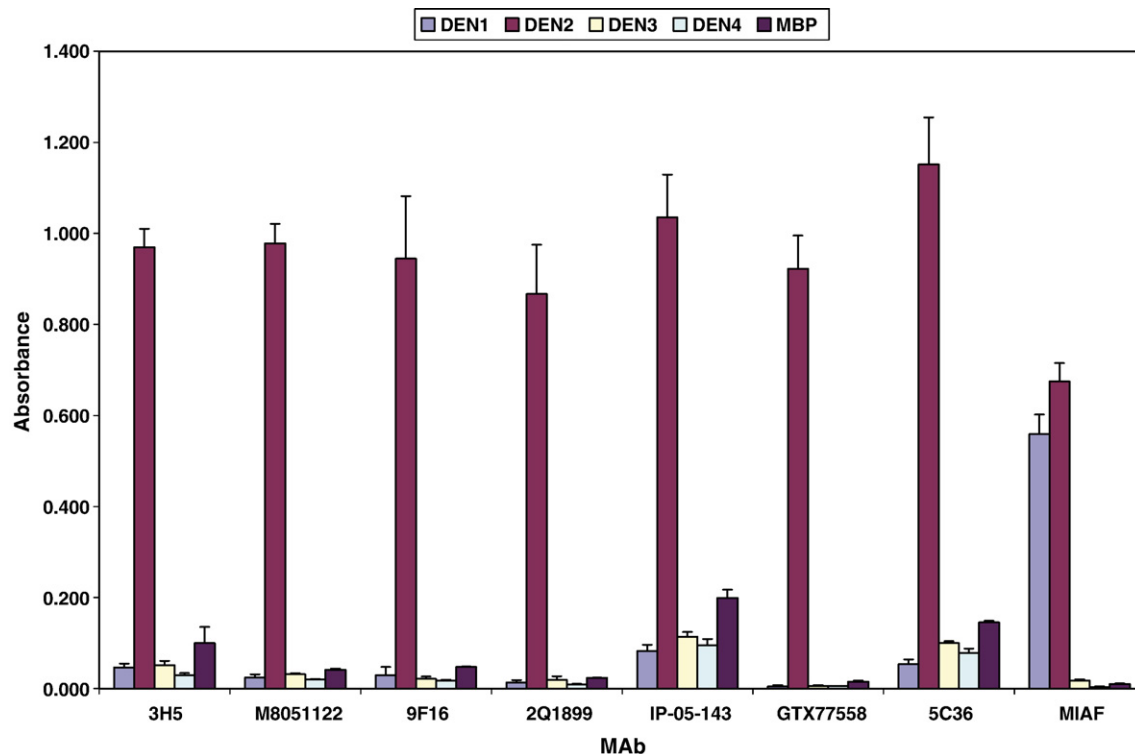


Fig. 2. ELISA showing the reactivity of the seven DENV-2 ED3 specific MAbs and DENV-2 MIAF with DENV-1, -2, -3, and -4 MBP-tagged rED3s and negative control MBP. MAbs were tested at a concentration 50-fold higher than their Kd for the DENV-2 NGC MBP-rED3. Equal loading for each of the proteins was confirmed with anti-MBP serum (data not shown). The error bars represent the standard deviation.

methods, and all had similar affinities for the DENV-2 NGC rED3 with Kds ranging from 0.9 nM to 4.3 nM (Table 1). Statistically significant differences in Kd values were seen between MAbs 3H5 and GTX77558, 3H5 and IP-05-143, as well as 2Q1899 and GTX77558.

To determine if the affinity of each MAb for the rED3 was similar to the affinity for virion-associated ED3, the Kd of each MAb was determined by titration in an indirect ELISA using purified DENV-2 NGC virus as antigen. The affinity of each MAb for the virion-associated ED3 was nearly identical to the affinity for the rED3, with Kd values ranging from 0.9 nM to 7.2 nM (Table 1). There were no statistically significant differences in Kd values between MAbs or between the Kd values for virion-associated ED3 and rED3 for each MAb. This indicates that the presentation of the rED3 bound to the solid

phase is equivalent to what is presented by virion-associated ED3.

A neutralization assay (using PRNT₅₀) was undertaken for each of the seven MAbs with DENV-2 strain NGC to determine the concentration of MAb required to obtain a 50% reduction in virus infectivity. The PRNT₅₀ concentrations ranged from 1.5 nM to 11.6 nM for all seven MAbs (Table 1). MAb 5C36 had a statistically significant difference in PRNT₅₀ concentration compared to the other six MAbs. This MAb required a slightly higher concentration (2-fold to 8-fold higher compared to the other six MAbs) to achieve a 50% reduction in virus infectivity. This observation did not correlate with the affinity of MAb 5C36 for rED3 or virion-associated ED3 as there was no statistical difference in affinity from the other 6 MAbs.

Table 1
Properties of DENV-2 MAbs

MAb clone	Isotype	DENV-2 strain raised against	DENV rED3 specificity	Kd with DENV-2 NGC rED3 (nM)	Kd with DENV-2 NGC virus (nM)	PRNT ₅₀ concentration (DENV-2 NGC) (nM)
3H5	IgG1	NGC	2	4.3±0.7	2.8±0.1	4.6±0.8
M8051122	IgG1	NGC	2	2.5±0.3	4.1±1.1	3.6±0.4
9F16	IgG1	NGC	2	3.2±0.3	4.1±0.7	5.2±0.8
2Q1899	IgG1	NGC	2	4.0±0.5	7.2±2.1	5.4±0.5
IP-05-143	IgG1	Unknown	2	1.8±0.2 ^a	3.0±0.5	5.0±0.6 ^a
GTX77558	IgG1	Unknown	2	0.9±0.1	0.9±0.4	1.5±0.2
5C36	IgG1	Unknown	2	2.2±0.2 ^b	3.9±0.3 ^b	11.6±1.2 ^b

^a There was a statistically significant difference between the Kd with rED3 and the PRNT₅₀ concentration for MAb IP-05-143.

^b There was a statistically significant difference between the Kd with rED3/virus and PRNT₅₀ concentration for MAb 5C36.

Neutralization of DENV-2 strains by MAb 3H5

MAb 3H5 was used, as an example, to examine the ability of a DENV-2 ED3 type-specific MAb to neutralize multiple DENV-2 strains. A total of five DENV-2 strains (NGC, DAKHD10674, DAKAR578, H8-2027, and IB-H11208) were tested in a PRNT₅₀ assay. MAb 3H5 effectively neutralized all five strains with PRNT₅₀ concentrations ranging from 2.3 nM to 7.4 nM (Table 2). There was no statistically significant difference between the PRNT₅₀ concentrations of any of the DENV-2 strains compared to DENV-2 NGC.

Occupancy of ED3 on the virion and neutralization of infectivity

According to the law of mass action, the relative occupancy is a function of the dissociation constant, Kd, and the concentration of un-complexed MAb. In both the ELISA and PRNT assays there was a molar excess of MAb. To illustrate this point, even if all of the approximately 5×10^4 PFU (i.e. virions) were capable of being bound to the wells in the ELISA plate, the molar ratio of MAb to virion-associated ED3 would still be about 130 at the lowest dilution of MAb used. This ratio would be at least two orders of magnitude higher with the 100 PFU used in the PRNT assays. Under these conditions, the complexed MAb becomes negligible and therefore the concentration of un-complexed MAb remains relatively constant. Therefore, the fractional occupancy as predicted by the ELISA using purified virus as antigen can be translated to the fractional occupancy of ED3 on virions by MAb in the PRNT assay (see Materials and methods).

For each MAb, the ELISA binding data with purified virus as antigen were translated to percent relative occupancy (see Materials and methods) and was compared to the curve of percent neutralization of virus infectivity as a function of MAb concentration. As examples, this comparison is shown for MAbs 3H5 and 5C36 (Figs. 3a and b, respectively). For MAb 3H5 the curve for relative occupancy of ED3 on the virion as a function of MAb concentration had a slope factor of -1.0 ± 0.0 and a Kd value of 2.8 ± 0.1 nM (Fig. 3a). By contrast, the curve for percent neutralization of virus infectivity as a function of MAb concentration had a slope factor of -1.5 ± 0.4 and a PRNT₅₀ concentration of 4.6 ± 0.8 nM (Fig. 3a). For Mab 5C36, the curve for relative occupancy of ED3 on the virion as a function of MAb concentration had a slope factor of -1.0 ± 0.0 and a Kd value of 3.9 ± 0.3 nM (Fig. 3b). By

contrast, the curve for percent neutralization of virus infectivity as a function of MAb concentration had a slope factor of -2.0 ± 0.4 and a PRNT₅₀ concentration of 11.6 ± 1.2 nM (Fig. 3b). The fact that the curves for physical binding and neutralization have different slopes indicates that neutralization of virus infectivity is correlated with, but not directly proportional to, MAb occupancy of ED3. A similar relationship between relative occupancy of ED3 on the virion and neutralization of virus infectivity was seen for the other five Mabs as well (curves not shown). For all the MAbs the data for binding to virion-associated ED3 were best fit by a standard ligand binding curve with a slope factor of -1.0 and the Kds for these curves are listed in Table 1. The data for neutralization of infectivity by all of the MAbs were best fit by dose-response curves having a variable slope factor, which in all cases was steeper than the slope factor for the curve of MAb binding to virion-associated ED3. The slope factors for neutralization were -1.5 ± 0.3 for MAb M8051122, -1.4 ± 0.3 for MAb 9F16, -2.2 ± 0.4 for MAb 2Q1899, -1.6 ± 0.3 for MAb IP-05-143, and -1.9 ± 0.4 for MAb GTX77558. The PRNT₅₀ concentrations for these MAbs are reported in Table 1.

The data for all seven MAbs were also plotted with percent neutralization of virus infectivity as a function of percent relative occupancy of ED3 on the virion. For all seven MAbs there was a linear relationship between the relative occupancy of ED3 required to neutralize the majority of virus infectivity ($\sim 90\%$). The data were fit by a line ($R^2 > 0.98$) and as examples MAb 3H5 is shown in Fig. 3c and MAb 5C36 in Fig. 3d. For MAb 3H5, the equation for the line is $y = 1.43x - 35.65$, where y = “percent neutralization of virus infectivity” and x = “percent relative occupancy of ED3 on the virion by MAb.” Using this model for MAb 3H5, it is predicted that at approximately 32%, 60%, and 88% occupancies of ED3 by MAb the percent neutralization of virus infectivity will be approximately 10%, 50%, and 90%, respectively (Fig. 3c). In addition, a threshold for neutralization is predicted from this model at approximately 25% occupancy of ED3 by MAb 3H5 (Fig. 3c). The results were strikingly different when the same analysis was done for MAb 5C36. It is predicted that at approximately 55%, 75%, and 94% occupancies of ED3 by MAb 5C36 the percent neutralization of virus infectivity will be approximately 10%, 50%, and 90%, respectively (Fig. 3d). In addition, a threshold for neutralization is predicted from this model at approximately 50% occupancy of ED3 by MAb 5C36 (Fig. 3d). The same analysis was done for the other five MAbs and estimates of percent relative occupancy predicted to neutralize various

Table 2
PRNT₅₀ concentrations of various DENV-2 strains with MAb 3H5

DENV-2 Strain	Host	Year isolated	Country where isolated	Genotype	PRNT ₅₀ concentration (nM)
NGC	Human	1944	New Guinea	Asian 2	4.6 ± 0.8
DAKHD10674	Human	1970	Senegal	Sylvatic	5.1 ± 0.7
DAKAR578	Mosquito	1980	Ivory Coast	Sylvatic	7.4 ± 0.4
H8-2027	Human	Unknown	Malaysia	ND ^a	4.3 ± 0.9
IB-H11208	Human	1966	Nigeria	ND ^a	2.3 ± 0.1

^a ND: not determined.

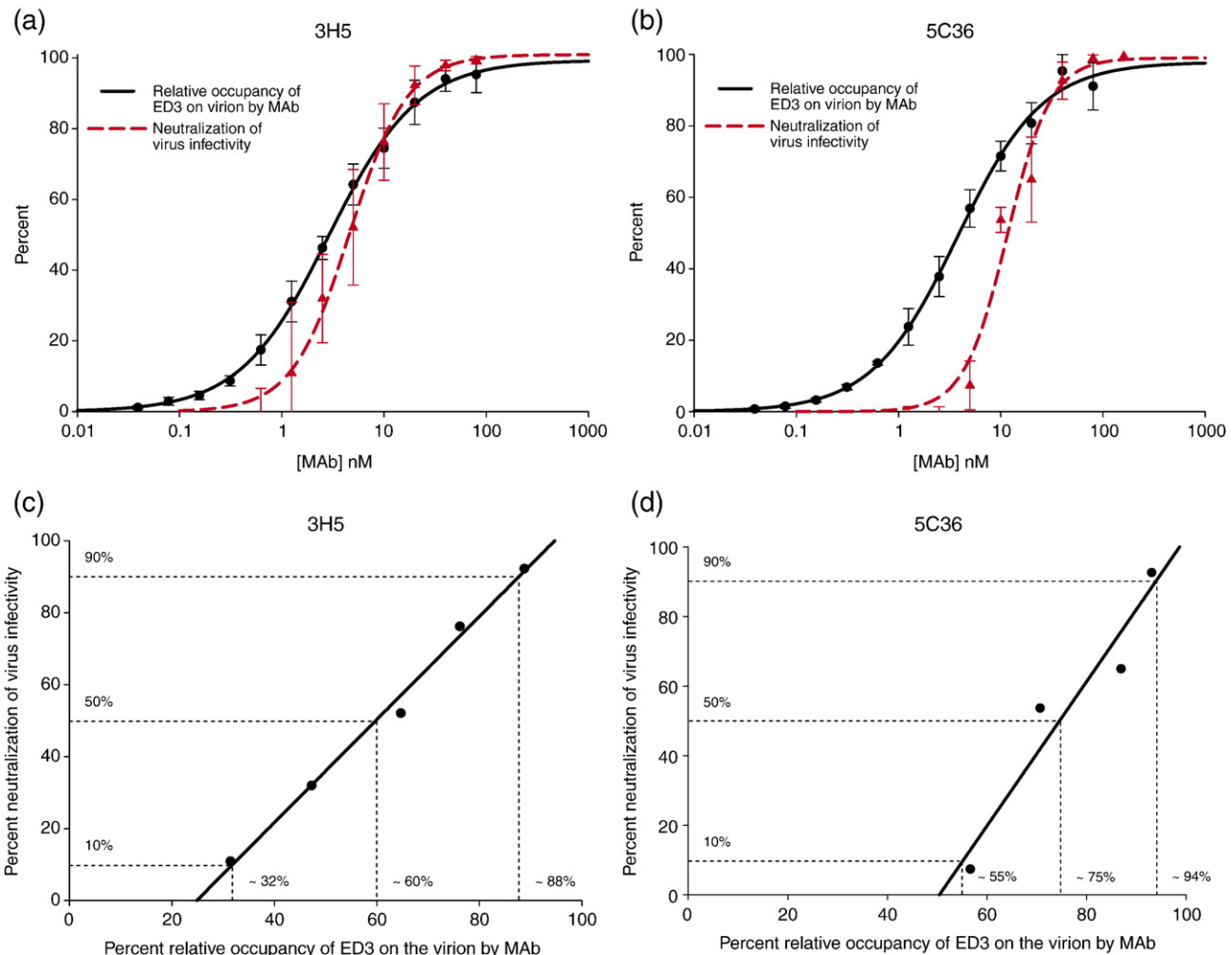


Fig. 3. Relationship between occupancy of ED3 binding sites and neutralization of virus infectivity using MAbs 3H5 and 5C36 as examples. Panels a and b are graphs comparing the percent relative occupancy of available ED3 binding sites on the DENV-2 virion by MAb and the percent neutralization of virus infectivity as a function of the concentration of MAb. As the occupancy of ED3 approaches saturation the percent neutralization of virus infectivity approaches 100%. The relative occupancy curves for both MAb 3H5 and MAb 5C36 have slope factors of -1.0 ± 0.0 whereas the neutralization curves have slope factors of -1.5 ± 0.4 for MAb 3H5 and -2.0 ± 0.4 for MAb 5C36. This indicates that occupancy and neutralization are correlated, but not proportionally. Panels c and d show the percentage of virus infectivity neutralized as a function of the percent relative occupancy of ED3 binding sites on the virion for MAbs 3H5 and 5C36. There is a linear relationship between occupancy and neutralization of the majority of virus infectivity ($\sim 90\%$) for both MAbs and from this model it is predicted that relative occupancies of $>25\%$ for MAb 3H5 or $>50\%$ for MAb 5C36 are necessary for virus neutralization.

percentages of virus infectivity are shown in Table 3. The widest range of relative occupancy values between MAbs was seen for the estimated thresholds of neutralization. MAbs that deviated furthest from the mean of $25\% \pm 5\%$ relative occupancy were M8051122 and 5C36, having thresholds for virus neutralization estimated at 10% and 50% respectively. The mean for 10% neutralization of virus infectivity was $32\% \pm 5\%$ relative occupancy and MAbs M8051122 and 5C36 differed the most from the mean with an estimated relative occupancy of 18% and 55%, respectively. The mean for 50% neutralization of virus infectivity was $59\% \pm 3\%$ relative occupancy with MAbs 2Q1899 and 5C36 deviating the most with estimated occupancies of 46% and 75%, respectively. The narrowest range of occupancy values between MAbs was seen for 90% neutralization of virus infectivity. The mean was $86\% \pm 3\%$ relative occupancy and MAbs 2Q1899 and 5C36 deviated the most,

Table 3
 Estimates of percent relative occupancy of ED3 on the virion by MAb required to neutralize various percentages of virus infectivity

MAb	Percent relative occupancy of ED3 on virion by MAb predicted to result in a percent neutralization of virus infectivity of			
	0% (threshold) ^a	10%	50%	90%
3H5	25%	32%	60%	88%
M8051122	10%	18%	51%	84%
9F16	15%	23%	55%	87%
2Q1899	16%	22%	46%	70%
IP-05-1432	28%	35%	60%	85%
GTX77558	31%	38%	64%	90%
5C36	50%	55%	75%	94%

^a Percent relative occupancy levels greater than the threshold value are predicted to neutralize virus infectivity.

Table 4

Relative dissociation constants of mutant rED3s compared to wild-type (Wt) NGC rED3 with all MAb/rED3 mutant combinations

rED3	DENV-2 Type-specific MAb						
	3H5	M8051122	9F16	2Q1899	IP-05-143	GTX77558	5C36
Wt	1.0	1.0	1.0	1.0	1.0	1.0	1.0
K295G	0.4	0.7	2.3	1.1	0.6	1.1	0.7
S298G	0.4	0.4	0.5	0.9	1.1	1.5	0.9
Y299I	0.5	0.4	0.5	0.9	1.0	1.3	1.0
S300L	0.9	0.7	1.0	2.0	0.9	1.3	0.9
M301G	≥19	≥32	≥25	≥20	≥45	≥47	20.0
M301A	1.5	2.4	1.8	1.9	2.5	4.5	2.7
T303G	1.0	0.7	0.7	1.4	1.2	2.2	1.2
K305G	13.0	16.0	≥25	≥20	14.0	≥47	15.0
K305A	≥19	31.0	≥25	≥20	≥45	≥47	≥72
K307G	1.1	1.2	4.4	3.3	1.5	2.1	1.8
V309G	1.4	1.0	1.1	1.8	1.3	2.1	1.0
K310E	0.3	0.6	1.6	0.9	0.7	0.7	0.5
E311G	0.7	0.6	0.6	1.7	0.8	1.5	0.9
E327G	0.5	0.6	4.2	1.5	1.0	1.5	0.5
D329E	4.1	2.5	2.1	3.6	0.9	1.4	1.2
D329G	0.6	0.6	4.5	0.9	0.9	0.7	0.5
G330D	0.4	0.4	0.4	0.7	0.8	1.1	0.5
S331A	0.3	0.6	1.4	1.0	1.0	1.1	0.7
S331P	2.2	1.3	1.2	2.2	0.9	1.1	1.1
P332G	7.1	3.0	2.6	6.6	2.1	4.2	3.1
P332A	5.4	1.3	0.9	0.2	0.5	6.3	4.9
K334Q	0.3	0.6	1.2	1.1	1.0	1.1	0.5
E338G	1.2	0.8	1.0	2.9	1.0	1.8	1.0
K344N	1.5	1.0	1.2	2.2	1.0	1.1	1.1
R345K	0.4	0.6	1.4	0.6	0.8	0.8	1.2
R345G	1.4	1.0	1.0	3.5	0.9	1.2	1.2
T359I	1.8	1.0	0.9	0.7	0.8	0.7	1.1
T359G	1.3	1.0	0.9	3.1	0.9	1.2	1.1
E360G	0.4	0.5	1.6	0.9	0.6	0.6	0.4
K361G	0.8	0.8	1.7	1.8	0.8	1.2	0.7
D362G	0.5	0.6	1.2	0.6	0.9	0.7	0.5
S363R	0.4	0.6	0.9	0.6	0.9	1.0	0.6
E383G	≥19	12.0	≥25	≥20	≥45	≥47	19.0
E383A	0.9	0.9	0.8	1.4	0.7	0.4	1.4
P384G	≥19	≥32	≥25	≥20	≥45	≥47	20.0
P384A	≥19	≥32	≥25	≥20	≥45	≥47	≥72
G385E	0.5	0.6	0.6	0.9	0.8	0.8	0.6
K388G	2.6	1.0	3.7	3.3	1.5	1.7	0.5
N390D	0.9	0.8	1.1	2.1	0.9	1.5	0.6
N390H	0.6	0.4	1.1	1.4	0.5	0.3	0.8
N390S	0.8	0.7	0.8	1.8	1.0	1.6	0.8

Significant changes in binding affinity relative to Wt are shown in bold.

having estimated relative occupancies of 70% and 94%, respectively.

Binding affinity of MAbs with rED3 mutants

A total of 41 single amino acid substitutions were introduced into the rED3 at 30 different surface accessible residues (Table 4). Surface accessibility was determined by examining the crystal structure of the DENV-2 E protein dimer (PDB-ID: 1OKE) (Modis et al., 2003). The solvent accessible surface area was calculated for individual residues from 295 to 395 of the DENV-2 ED3 using the program GETAREA 1.1 (Fraczkievicz and Braun, 1998). Residues with 20% to 50% solvent accessibility were considered to be moderately accessible and

these residues were mutated only if a naturally occurring DENV-2 substitution was identified at that site (see below). Greater than 50% accessibility was considered highly accessible and all the residues that fell into this category were mutated. VIPERdb (Shepherd et al., 2006) was used to confirm that residues calculated to be solvent accessible by GETAREA 1.1 were also accessible on the surface of the virus based on the cryo-EM model of the mature DENV-2 virion (PDB-ID: 1THD) (Zhang et al., 2003).

The ED3 sequence (residues 295–395 of E) of 50 DENV-2 strains were aligned in order to identify amino acid substitutions of surface accessible residues (according to the parameters listed above) relative to DENV-2 strain NGC. These 50 DENV-2 strains are representatives of all six of the currently described DENV-2 genotypes (Rodriguez-Roche et al., 2005) and likely represent the majority of surface accessible amino acid sequence diversity within ED3 for DENV-2. A total of seventeen naturally occurring substitutions were identified at fourteen surface accessible residues (Fig. 4) and these were individually incorporated into the rED3. In addition, 16 conserved residues were identified (Fig. 4) as being highly surface accessible and were subjected to a combination of glycine and alanine scanning mutagenesis, essentially to remove the side chain of each residue. Initially, glycine substitutions were used for all conserved residues, as well as instances when there was a very conservative natural substitution. Glycine substitutions that resulted in greater than 4-fold changes in MAb binding affinity for more than one of the MAbs tested were also mutated to alanine to verify the results. The reasoning for this approach was that glycines, with only a hydrogen atom as a side chain, have more conformational freedom than any other residue and could therefore increase the conformational entropy in parts of the protein where they were substituted (Branden and Tooze, 1999), which alone could affect MAb binding affinity. This was thought to be a good initial indicator for critical epitope residues as the affinity change would potentially be more dramatic. In addition, preliminary studies indicated that glycine substitutions of surface residues were well tolerated in the rED3 based on MAb affinity measurements. Alanine, however, is constrained by a side chain and therefore does not have the same conformational freedom as glycine and was used to verify initial mapping of potential epitope residues based on a glycine substitution.

The Kd of the seven DENV-2 type-specific MAbs was determined by titration in an indirect ELISA with all 41 rED3 mutant proteins. Most amino acid substitutions had a relatively minor effect on the binding affinity of all seven MAbs, having less than a 4-fold change compared to the wild-type rED3 (Table 4). Those substitutions that resulted in a change in binding affinity between 4- and 10-fold were defined as having “weak” affects on the binding affinity. For MAb 3H5 mutants D329E, P332G, and P332A fell into this category. With MAb 9F16 mutants K307G, E327G, and D329G had weak affects on binding affinity. Only mutant P332G had a weak affect on the binding affinity of MAb 2Q1899. Mutants M301A, P332G, and P332A had weak affects on the binding affinity of MAb

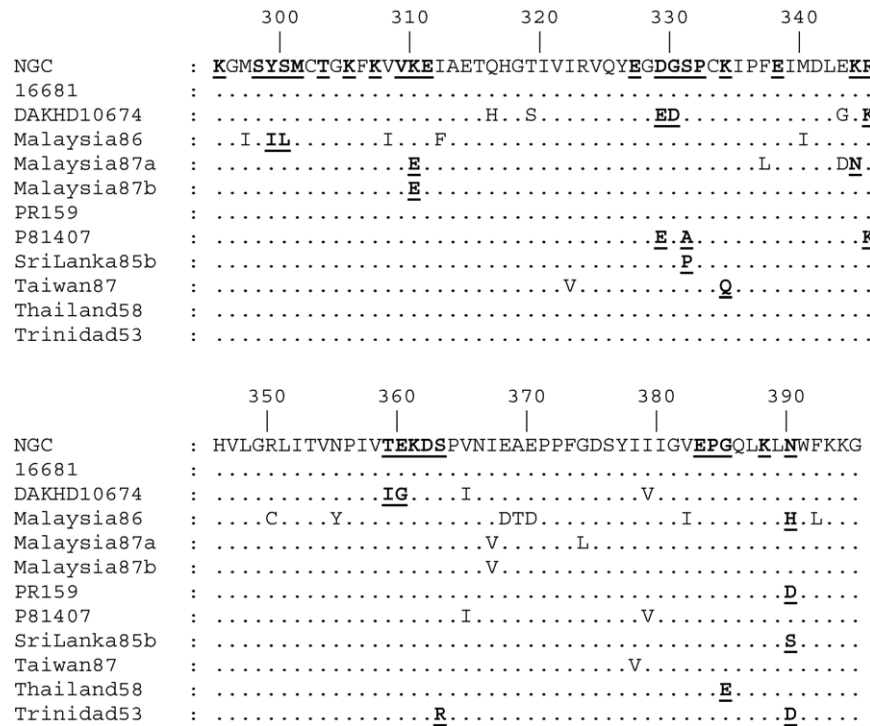


Fig. 4. DENV-2 ED3 alignment of 11 representative strains compared to DENV-2 NGC. Naturally occurring amino acid substitutions and conserved residues which were mutated to glycine/alanine are in bold and underlined. All the residues that were mutated are surface accessible residues on the DENV-2 virion. The DENV-2 NGC and DAKHD10674 sequences were done by the authors, the Malaysia 87a sequence is from Samuel et al. (1989), and the rest were acquired from GenBank; 16681 (U87411), Malaysia86 (X15433), Malaysia87b (X15434), PR159 (L10046), P81407 (AF231717), SriLanka85b (L10040), Taiwan87 (L10052), Thailand58 (D10514) and Trinidad53 (L10053).

GTX77558. Lastly, mutant P332A weakly affected the binding affinity of MAb 5C36 and no mutants fell into this category for MAbs M8051122 and IP-05-143.

Mutations that resulted in a greater than 10-fold change in binding affinity were considered to have “strong” affects. These were M301G, K305G, K305A, E383G, P384G, and P384A. All six of these had similar effects on binding affinity for the seven MAbs tested (Table 4). Discrepancies in the results occurred with mutants M301G and M301A, as well as E383G and E383A. In these two cases there was a greater than 10-fold decrease in binding affinity with the glycine mutant but no change with the alanine mutant. This would imply that residues M301 and E383 are not critical for the interaction of these MAbs with ED3 but are still likely to be located on the periphery of the epitope. MAb GTX77558 was an exception and showed a weak decrease in binding affinity with mutant M301A indicating that residue M301 may be more important for the binding of this MAb to ED3.

Epitope analysis

Mutations M301G, K305G, K305A, E383G, P384G, and P384A resulted in greater than 10-fold decreases in binding affinity with all seven MAbs as compared to the wild-type rED3. Residues M301, K305, E383, and P384 are found on two adjacent loops and cluster relatively close to one another on the upper lateral face of ED3 (Fig. 5a). As stated above, residues M301 and E383 do not appear to be critical for MAb binding as

M301A and E383A mutations had no effect on the binding affinity of any of the MAbs with the exception of MAb GTX77558, which showed weak loss of binding with mutant M301A. Therefore, residues K305 and P384 are the critical amino acids involved in the antigenic site of all seven MAbs tested (Fig. 5a, shown in red).

Mutations that were considered to have “weak” affects on binding of one or more of the seven MAbs were M301A, K307G, E327G, D329E, D329G, P332G, and P332A. Consequently, these residues are predicted to be located on the periphery of the MAb epitopes (Fig. 5a, shown in pink). Residues M301 and E383 are considered to be on the periphery of the epitope for all seven MAbs as they are adjacent to other critical residues and their affect on the binding affinity was dependant on the substitution (Fig. 5a, shown in pink).

The epitope mapping data suggest that there are four similar, overlapping, epitopes recognized by the seven DENV-2 ED3 type-specific MAbs in this study that form one major antigenic site. All four epitopes are composed of the same two critical residues (K305 and P384) as well as two peripheral residues (M301 and E383) but have distinct footprints on ED3 as evidenced by the variable “weak” loss of binding with certain mutants (Fig. 5b). Peripheral residues for MAb 3H5 include D329 and P332 while for MAb 9F16 residues K307, E327, and D329 are likely to be found on the periphery of the epitope. MAbs 2Q1899, GTX77558, and 5C36 have residue P332 on the periphery of the epitope they recognize. However, for MAbs M8051122 and IP-05-143 no additional residues

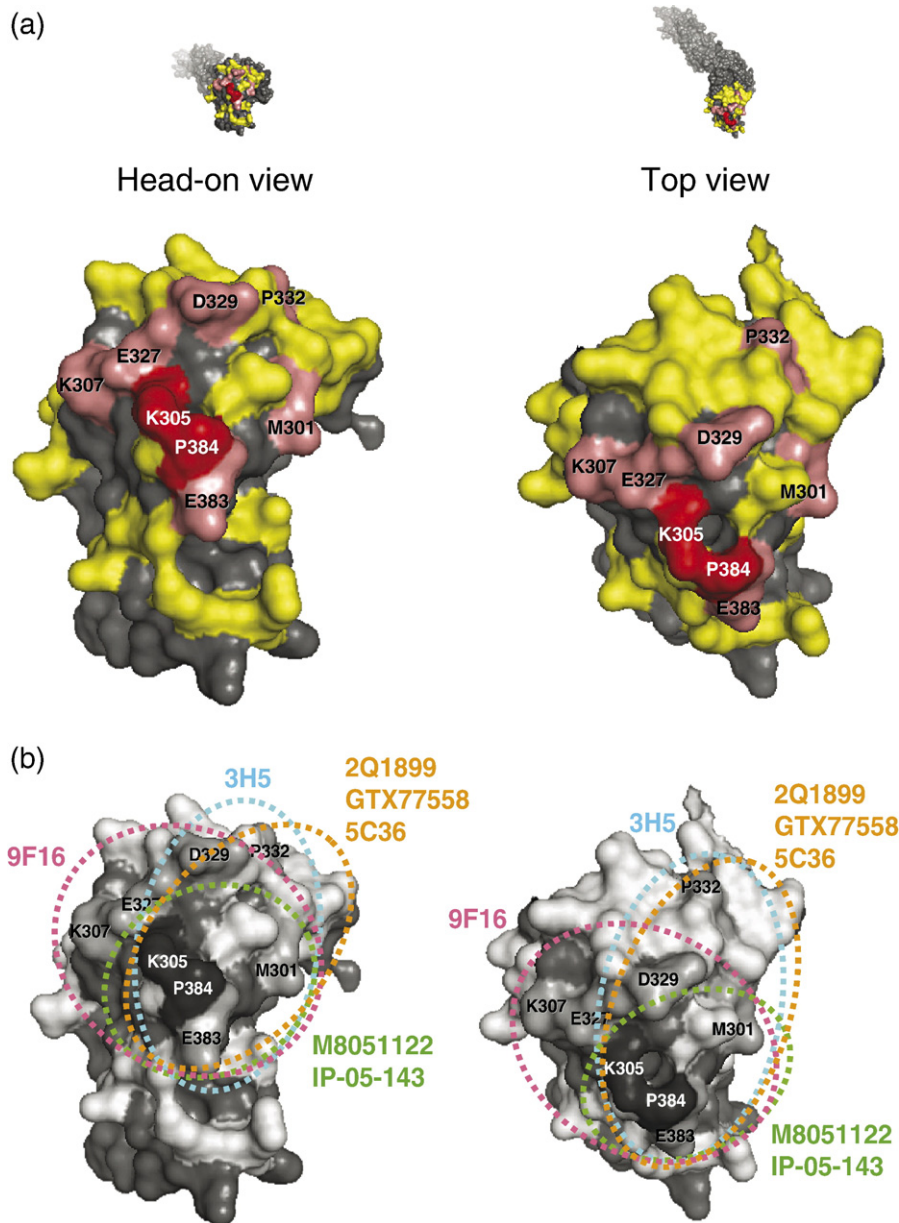


Fig. 5. Predicted epitope for the seven MAbs in this study. (a) All the mutated residues are colored yellow. Residues K305 and P384 are predicted to form the center of the epitope of all seven MAbs and are colored red. Residues M301 and E383 are predicted to be on the periphery of the epitope for all seven MAbs and are colored pink. Different combinations of residues K307, E327, D329, and P332 are predicted to be on the periphery of subsets of the seven MAb epitopes and also are colored pink. (b) There are predicted to be four overlapping epitopes recognized by the seven MAbs and these epitopes center on the critical residues K305 and P384. The rings represent the area predicted to be the footprint of each MAb or set of MAbs on the surface of ED3 as predicted by their interaction with peripheral residues. The 3H5 epitope is shown in blue and includes residues M301, E383, D329, and P332. The 9F16 epitope is shown in purple and includes residues M301, K307, E383, E327, and D329. The epitope recognized by MAbs 2Q1899, GTX77558, and 5C36 is shown in gold and includes residues M301, E383, and P332. The epitope for MAbs M8051122 and IP-05-143 is shown in green and includes residues M301 and E383. The diagrams are based on the crystal structure of the DENV-2 E protein (PDB-ID: 1OKE).

were identified as being on the periphery of the epitope that they recognized.

Discussion

The goal of this study was to characterize the epitopes recognized by seven DENV-2 ED3 type-specific MAbs. Site-directed mutagenesis was employed to generate a panel of DENV-2 NGC rED3 mutants containing single amino acid

substitutions of surface accessible residues. The results obtained reveal that the seven MAbs recognize overlapping epitopes that form one antigenic site. It would appear that this antigenic site is a dominant DENV-2 neutralization determinant, a concept that is consistent with studies on other flaviviruses (Roehrig, 2003).

Previous studies have attempted to map the epitope of MAb 3H5 (Hiramatsu et al., 1996; Trirawatanapong et al., 1992) and produced conflicting results. Our results partially agree with those of Hiramatsu et al. (1996) who described a contiguous

epitope for MAb 3H5 composed of residues 383–385 of the E protein using a DENV infectious clone containing the prM and E genes of DENV-2 NGC. Our results, however, indicate that only residue P384 is a critical residue within the epitope, while we predict that residue E383 is on the periphery of the epitope. Also, using a very non-conservative G385E mutant rED3, we saw no loss in binding affinity with MAb 3H5 indicating that this residue is not part of the epitope. In addition, our results indicate that the epitopes recognized by all seven MAbs, including 3H5, are conformational as the critical residues (K305 and P384) for binding are located on adjacent, discontinuous segments of ED3. Several additional residues are predicted to be on the periphery of the MAb epitopes and indicate that their footprints on ED3 cover at least three discontinuous segments. These segments include a section of the N-terminal linker region through a portion of β-strand A (residues 301–307), parts of the BC loop region (residues 327–332), and FG loop residues 383 and 384, which come together to form a single antigenic site on the upper surface and lateral face of ED3. This is consistent with data from studies with other flaviviruses, namely WNV (Nybakken et al., 2005) and JEV (Wu et al., 2003), and could indicate that similar type-specific neutralizing epitopes exist on the equivalent surfaces of ED3 of DENV-1, -3, and -4.

The antigenic site recognized by the MAbs in this study seems to be highly conserved among DENV-2 strains and is, therefore, a potentially very important component of candidate DENV-2 vaccines. Surprisingly, only 1 of the 17 naturally occurring rED3 mutants (D329E) affected MAb binding. This mutation only resulted in a weak (4-fold) decrease in binding affinity for one MAb (3H5). Conservation of this DENV-2 type-specific antigenic site was confirmed by MAb 3H5, which was used as a representative of the seven MAbs studied and was shown to efficiently neutralize five different DENV-2 strains with very similar PRNT₅₀ concentrations. One of these strains, DAKHD10674, contains the D329E mutation that caused a weak decrease in affinity of MAb 3H5 for the rED3. This verifies our assessment of the substitution of residues deemed to be critical epitope residues and those considered to be on the periphery. The overall conservation of this antigenic site may indicate its importance as a functional epitope for the virus.

The initial attachment of DENV and other flaviviruses to mammalian and mosquito cell lines, in-vitro, has been shown to depend on cell surface glycosoaminoglycans, in particular heparan sulfate (Chen et al., 1997; Hung et al., 1999). Soluble heparin has been shown to block the binding of DENV-2 ED3 to BHK21 cells, which suggests that ED3 binds to cell surface heparan sulfates (Hung et al., 2004). The putative heparan sulfate binding site on the DENV-2 ED3 includes residues K305, K307, and K310 (Hung et al., 2004). Therefore, one proposed mechanism of neutralization by the DENV-2 type-specific MAbs used in this study is by blocking ED3 attachment to cell surface heparan sulfates as a result of MAb binding to residue K305 by all seven MAbs, and also to K307, which was predicted to be on the periphery of the epitope of MAb 9F16. Heparin, however, was not shown to block the binding of ED3 to C6/36 mosquito cells, but a DENV-2 E peptide comprising

residues 380–389 of ED3 did (Hung et al., 2004). Since our predicted epitope for the seven MAbs tested includes residue P384, it would follow that these MAbs would also block attachment of ED3 to a yet unidentified mosquito cell receptor as well. Thus, the location of the antigenic site recognized by all seven DENV-2 MAbs in this study supports a mechanism of neutralization that, at least in part, entails blocking of attachment to cell receptor.

Our results indicate that, as the available ED3 binding sites on the virion are saturated by MAb, neutralization of virus infectivity approaches 100%. Virus neutralization was observed to increase incrementally as a result of increased MAb occupancy of ED3, which implies that occupancy levels below 100% probably reduce the propensity of individual virus particles to successfully infect susceptible cells. This is most likely due to competition between MAbs and cell surface receptors for binding to ED3 on virions since neutralizing MAbs against ED3 have been shown to efficiently block virus adsorption to susceptible cells (Crill and Roehrig, 2001). In addition, depending on the MAb, it is predicted that 10%–50% relative occupancy of ED3 on the virion by MAb is necessary for virus neutralization and for all seven MAbs occupancy levels approaching saturation were required for 100% neutralization of virus infectivity. This corresponds to a multi-hit mechanism of neutralization, which has been described for several other viruses including rabies virus (Flamand et al., 1993), poliovirus (Icenogle et al., 1983), rhinovirus (Smith et al., 1993), adenovirus (Stewart et al., 1997), papillomavirus (Booy et al., 1998), and influenza virus (Taylor et al., 1987).

Variability was seen between the MAbs with respect to the relative occupancy levels predicted to neutralize particular percentages of virus infectivity (Table 3). This was significant as all seven MAbs recognize overlapping epitopes that form one antigenic site on ED3. Although four overlapping epitopes were identified by the seven MAbs, the differences in occupancy levels required for neutralization of virus infectivity did not necessarily correlate with MAbs that recognized similar epitopes. This implies that there are inherent differences between the interactions of MAbs with ED3 that allow some to neutralize more effectively at lower relative occupancy levels. This is especially true for MAb 5C36, which neutralized the majority of virus infectivity over a relatively narrow range of occupancies (50%–94%) compared to the other six MAbs yet all had similar affinities for virion-associated ED3. Clearly, more studies are necessary to understand the mechanism of neutralization of DENV-2.

An improved understanding of the neutralization mechanism of DENV-2 by anti-ED3 antibodies will allow for a vaccine design that will elicit the most potent neutralizing antibody responses. In this study four overlapping neutralizing epitopes were identified that appear to form a single, dominant, antigenic site on ED3 that is conserved among DENV-2 strains. The relative occupancy of this antigenic site by MAbs was correlated with neutralization of virus infectivity and indicated that anti-ED3 type-specific MAbs neutralized virus particles primarily by saturating available ED3 binding sites. Overall, designing a vaccine that elicits antibodies to this dominant

DENV-2 ED3 type-specific neutralization determinant in humans would be advantageous and could be expected to protect against all known DENV-2 strains.

Materials and methods

Cells and viruses

Monkey kidney Vero cells were maintained at 37 °C in a 5% CO₂ incubator in Dulbecco's modified essential media (DMEM) containing 8% fetal bovine serum (FBS). Mosquito C6/36 cells were maintained at 28 °C in DMEM containing 10% FBS and supplemented with tryptose phosphate buffer. The DENV strains used in this study were DENV-2 New Guinea C (NGC), S16803, DAKHD10674, DAKAR578, H8-2027, and IB-H11208 (Table 2). Primary virus stocks were passaged twice in C6/36 mosquito cells to obtain sufficient titers.

Purification of virus

C6/36 mosquito cells were grown in a 850 cm² roller bottle and infected with DENV-2 NGC at an MOI of approximately 0.1. The cell infected supernatant was harvested on day 7 post infection. Cell debris was removed by centrifugation at 5000 rpm for 30 min at 4 °C. The supernatant was layered on top of a 30% sucrose solution containing 10 mM Tris, 100 mM NaCl, and 1 mM EDTA. The virus was pelleted by ultracentrifugation in a swinging bucket rotor at 26,000 rpm for 4 h at 4 °C to remove low molecular weight contaminants such as soluble proteins. The supernatant was poured off and the tubes were briefly left upside down on chromatography paper in order to remove excess liquid from the side of the tubes. The virus pellet was resuspended in PBS. The infectious titer was determined by a standard plaque assay on Vero cells. The purity of the virus preparations was verified by SDS-PAGE (data not shown).

MAbs

Seven commercially available MAbs were used in this study: 3H5 (Chemicon) (Gentry et al., 1982), M8051122 (Fitzgerald Industries), 9F16 (US Biological), 2Q1899 (US Biological), 5C36 (US Biological), IP-05-143 (RayBiotech, Inc.), and GTX77558 (GeneTex). All seven are affinity purified IgG1 mouse MAbs prepared against DENV-2.

Expression and purification of recombinant DENV-2 ED3

The region corresponding to ED3 of the DENV-2 strain New Guinea C (NGC) was reverse transcription-PCR amplified for cloning and expression as maltose binding protein (MBP) fusions using the pMal-c2x system (New England Biolabs, Beverly, MA). RNA extraction of virus infected cell culture supernatant was done using Qiagen Viral RNA extraction Kit (Qiagen). Reverse transcription-PCR was done using the Titan Kit (Roche). The primers used (Forward: 5'-CGAGGGAA-GGATTCAAAAGGAATGTCATACTCTATG -3' and

Reverse: 5'-GCCAAGCTTCATCCTTCTTAAACCAGTT-GAGC-3') were designed for cloning into the pMal-c2x vector and contained *Xmn*I and *Hind*III restriction sites respectively. Appropriate primers were also designed for constructing rED3s for DENV-1 strain OBS7690, DENV-3 strain H87, and DENV-4 strain 703-4 and these gene fragments were also cloned into pMal-c2x. The recombinant ED3s (rED3), comprising amino acids 295–395 of the E protein tagged to MBP, was expressed in *Escherichia coli* DH5α using a method similar to that described previously by Li et al. (2005). Briefly, 20 mL cultures of bacteria were grown in LB medium containing 50 µg/mL ampicillin to an OD600 of approximately 0.6 and induced with 1 mM IPTG at 37 °C for 3 h. Bacterial cells were pelleted and stored at –20 °C overnight. The following day cells were lysed in 1 mL of MBP column buffer (20 mM Tris–HCl, 200 mM NaCl, 1 mM EDTA) by freeze/thawing in liquid nitrogen/37 °C waterbath. Lysates were centrifuged at 12,000 rpm at 4 °C for 30 min and the supernatant was mixed with 500 µL amylose resin (NEB) in a 1.5 mL eppendorf and incubated at 4 °C on a rocker for 1 h. Tubes were centrifuged at 3000 rpm for 1 min and the supernatant removed. The resin was washed three times with 1 mL MBP column buffer and bound protein was eluted twice with 500 µL of MBP column buffer containing 10 mM maltose. Concentrations of proteins were determined by spectrophotometric analysis.

Mutagenesis of recombinant DENV-2 ED3

Site-directed mutagenesis of the DENV-2 NGC ED3 gene fragment in the pMal-c2x vector was done using the Quickchange kit (Stratagene, La Jolla, CA) according to the manufacturer's instructions.

Western blot

MAbs were initially tested for their reactivity with the DENV-2 rED3 by Western blot. The DENV-2 rED3 was expressed and extracted as described above. Crude bacterial lysates were run out in a 10% SDS polyacrylamide gel for both IPTG induced and uninduced (no expression of MBP tagged rED3) samples. The gel was either stained with brilliant blue R concentrate (Sigma) or transferred to a PVDF membrane for subsequent Western blotting with the DENV-2 MAbs at a dilution of 1/1000. Binding of these MAbs to the MBP tagged rED3 was detected using HRP conjugated goat anti-mouse immunoglobulins (Sigma) and detected using 3,3'-diaminobenzidine enhanced liquid substrate system according to the manufacturer's instructions (Sigma).

Indirect ELISA

An indirect ELISA was used to investigate the specificity of the DENV-2 MAbs. Briefly, 200 ng of MBP tagged rED3s from DENV-1 strain OBS7690, DENV-2 strain NGC, DENV-3 strain H87, and DENV-4 strain 703-4, as well as MBP alone was adsorbed to the wells of a 96-well microtiter plate in triplicate for each MAb. The MAbs were tested at a concentration that

was 50-fold higher than its Kd for the DENV-2 NGC rED3. In addition, a DENV-2 polyclonal mouse immune ascitic fluid (MIAF) was used as a positive control. The indirect ELISA was carried out in a similar manner to the affinity measurements by indirect ELISA (see below) except that Mabs were tested for binding at a single MAb concentration.

Plaque reduction neutralization test 50% (PRNT₅₀)

MAbs were diluted to either 80 nM (GTX77558), or 160 nM (3H5, M8051122, 9F16, 2Q1899, and IP-05-143), or 320 nM (5C36) and then serially diluted 2-fold in MEM containing 2% FBS to essentially cover the same range of concentrations as the affinity ELISA once diluted with an equal volume of virus. DENV-2 NGC was diluted to approximately 1 pfu/μL in MEM containing 2% FBS. 400 μL of virus (~400 pfu) was mixed with an equal volume of MAb dilution or 400 μL of MEM containing 2% FBS (control) and was incubated at room temperature (25 °C) for 1 h. Following this incubation, 200 μL of each virus/MAb mixture, or controls, was added in triplicate to wells of a 6-well plate containing ~80% confluent monkey kidney Vero cells. Infection was allowed to take place for 1 h at room temperature at which point the cells were washed twice with PBS, overlaid with MEM containing 2% FBS and 1% Agar, and incubated at 37 °C. Plaques were visualized on day 6 by staining with neutral red. PRNT data were converted to percent neutralization relative to controls in the absence of MAb and PRNT₅₀ concentrations were calculated by doing a non-linear regression analysis using SigmaPlot (Version 9.01, Systat Software, Inc., CA). The data are fitted by a standard four parameter logistic curve (i.e. dose-response curve) by the equation: $y = \min + (\max - \min) / (1 + (x/EC_{50})^{\text{slope factor}})$. PRNT₅₀ assays were carried out and analyzed in the same way for MAb 3H5 with DENV-2 strains S16803, DAKHD10674, DAKAR578, H8-2027, and IB-H11208 in addition to NGC. The results are an average of two experiments.

Affinity measurements by indirect ELISA with rED3

The wells of 96-well microtiter plates (Corning Inc., Corning, NY) were coated with 200 ng of rED3 diluted in borate saline pH 9.0 at 37 °C for 2 h. This amount of rED3 was determined to saturate the wells by undertaking a checkerboard serial dilution of anti-MBP antisera (NEB) and rED3, which yielded peak absorbance values that were below the maximum range of the plate reader (data not shown). Wells were washed twice with distilled and deionized water (ddH₂O) and blocked for 30 min at room temperature (25 °C) with blocking buffer [phosphate-buffered saline (PBS), 0.1% (v/v) Tween-20, 0.25% (w/v) bovine serum albumin (BSA)] and subsequently washed twice with ddH₂O. The DENV-2 Mabs were diluted to either 40 nM (GTX77558), or 80 nM (3H5, M8051122, 9F16, 2Q1899, IP-05-143), or 160 nM (5C36) and added to duplicate wells followed by 11 two-fold serial dilutions in blocking buffer. This range of concentrations was determined to cover the full range of binding, from undetectable binding to saturation, to the DENV-2 NGC rED3. Antibodies were allowed to bind overnight at room temperature (25 °C) for 15–18 h. Subsequently, the microtiter

plates were washed twice with ddH₂O and twice with PBS-T (PBS containing 0.1% Tween-20) followed by addition of a 1/1000 dilution of HRP conjugated goat anti-mouse immunoglobulins (Sigma) and incubated for 1 h at room temperature. Following this incubation microtiter plates were washed twice with ddH₂O and twice with PBS-T. Antibody binding was visualized by addition of 3,3',5,5'-tetramethylbenzidine substrate (Sigma). After 30 min of incubation at room temperature the absorbance was read at 655 nm on a model 3550-UV plate reader (Bio-Rad, Hercules, CA). Binding curves and Kd values were determined by doing a non-linear regression analysis using SigmaPlot (Version 9.01, Systat Software, Inc., CA). The results are an average of two experiments.

Affinity measurements and estimates of occupancy by antibody-sandwich ELISA with purified virus

The wells of a 96-well microtiter plate (Corning Inc., Corning, NY) were coated with 50 μL of a 1/5 dilution of rabbit anti-DENV-ED3 polyclonal sera (“capture antibody”) for 2 h at 37 °C. The plates were washed twice with PBS-T and twice with ddH₂O. Purified DENV-2 NGC (~5 × 10⁷ PFU/mL) was diluted 1/50 in blocking buffer and 50 μL was added to each well and incubated at 37 °C for 2 h. The remainder of the assay was undertaken as described above with the rED3, except that the primary Mabs were only incubated for 1 h at room temperature in accordance with the length of incubation used for the virus neutralization assay. The entire experiment was carried out in a biological safety cabinet as the virus was presumed to be infectious throughout the experiment. Binding curves and Kd values were determined by doing a non-linear regression analysis using SigmaPlot (Version 9.01, Systat Software, Inc., CA). The results are an average of two experiments. Generation of colored substrate, and thus the absorbance reading in the indirect ELISA, is proportional to the amount of antibody bound to antigen in the well. At saturation (i.e. maximum absorbance) it is predicted that all possible ED3 binding sites on the virion are occupied by MAb. Therefore, absorbance readings below saturation can be calculated as fractional occupancies of the total available ED3s by MAb.

Statistical analysis

The Kd values and PRNT₅₀ concentrations are presented as mean ± standard error of the mean (SEM) and were analyzed using SigmaStat (Version 3.1, Systat Software, Inc., CA). Statistical analyses were done using one-way analysis of variance (ANOVA) followed by a Bonferroni post hoc test with $P < 0.05$ required for statistical significance.

Acknowledgments

The authors would like to thank Dr. David W. C. Beasley for critically reviewing the manuscript. This work was supported by the Pediatric Dengue Vaccine Initiative. GDG is supported by a NIAID T32 predoctoral fellowship (AI07526).

References

- Allison, S.L., Schalich, J., Stiasny, K., Mandl, C.W., Kunz, C., Heinz, F.X., 1995. Oligomeric rearrangement of tick-borne encephalitis virus envelope proteins induced by an acidic pH. *J. Virol.* 69, 695–700.
- Allison, S.L., Schalich, J., Stiasny, K., Mandl, C.W., Heinz, F.X., 2001. Mutational evidence for an internal fusion peptide in flavivirus envelope protein. *E. J. Virol.* 75, 4268–4275.
- Booy, F.P., Roden, R.B., Greenstone, H.L., Schiller, J.T., Trus, B.L., 1998. Two antibodies that neutralize papillomavirus by different mechanisms show distinct binding patterns at 13 Å resolution. *J. Mol. Biol.* 281, 95–106.
- Branden, C., Tooze, J., 1999. "Introduction to Protein Structure." Garland Publishing, Inc., New York. pp. 9–10 and 356–357.
- Chambers, T.J., Hahn, C.S., Galler, R., Rice, C.M., 1990. Flavivirus genome organization, expression, and replication. *Annu. Rev. Microbiol.* 44, 649–688.
- Chen, Y., Maguire, T., Hileman, R.E., Fromm, J.R., Esko, J.D., Linhardt, R.J., Marks, R.M., 1997. Dengue virus infectivity depends on envelope protein binding to target cell heparan sulfate. *Nat. Med.* 3, 866–871.
- Crill, W.D., Roehrig, J.T., 2001. Monoclonal antibodies that bind to domain III of dengue virus E glycoprotein are the most efficient blockers of virus adsorption to Vero cells. *J. Virol.* 75, 7769–7773.
- Flamand, A., Raux, H., Gaudin, Y., Ruigrok, R.W., 1993. Mechanisms of rabies virus neutralization. *Virology* 194, 302–313.
- Fraczkiewicz, R., Braun, W., 1998. Exact and efficient analytical calculation of the accessible surface areas and their gradients for macromolecules. *J. Comput. Chem.* 19, 319–333.
- Gentry, M.K., Henchal, E.A., McCown, J.M., Brandt, W.E., Dalrymple, J.M., 1982. Identification of distinct antigenic determinants on dengue-2 virus using monoclonal antibodies. *Am. J. Trop. Med. Hyg.* 31, 548–555.
- Halstead, S.B., 1988. Pathogenesis of dengue: challenges to molecular biology. *Science* 239, 476–481.
- Heinz, F.X., Allison, S.L., 2000. Structures and mechanisms in flavivirus fusion. *Adv. Virus Res.* 55, 231–269.
- Hiramatsu, K., Tadano, M., Men, R., Lai, C.J., 1996. Mutational analysis of a neutralization epitope on the dengue type 2 virus (DEN2) envelope protein: monoclonal antibody resistant DEN2/DEN4 chimeras exhibit reduced mouse neurovirulence. *Virology* 224, 437–445.
- Hung, S.L., Lee, P.L., Chen, H.W., Chen, L.K., Kao, C.L., King, C.C., 1999. Analysis of the steps involved in dengue virus entry into host cells. *Virology* 257, 156–167.
- Hung, J.J., Hsieh, M.T., Young, M.J., Kao, C.L., King, C.C., Chang, W., 2004. An external loop region of domain III of dengue virus type 2 envelope protein is involved in serotype-specific binding to mosquito but not mammalian cells. *J. Virol.* 78, 378–388.
- Icenogle, J., Shiwen, H., Duke, G., Gilbert, S., Rueckert, R., Anderegg, J., 1983. Neutralization of poliovirus by a monoclonal antibody: kinetics and stoichiometry. *Virology* 127, 412–425.
- Kaufmann, B., Nybakken, G.E., Chipman, P.R., Zhang, W., Diamond, M.S., Fremont, D.H., Kuhn, R.J., Rossmann, M.G., 2006. West Nile virus in complex with the Fab fragment of a neutralizing monoclonal antibody. *Proc. Natl. Acad. Sci. U.S.A.* 103, 12400–12404.
- Kuhn, R.J., Zhang, W., Rossmann, M.G., Pletnev, S.V., Corver, J., Lenches, E., Jones, C.T., Mukhopadhyay, S., Chipman, P.R., Strauss, E.G., Baker, T.S., Strauss, J.H., 2002. Structure of dengue virus: implications for flavivirus organization, maturation, and fusion. *Cell* 108, 717–725.
- Lin, B., Parrish, C.R., Murray, J.M., Wright, P.J., 1994. Localization of a neutralizing epitope on the envelope protein of dengue virus type 2. *Virology* 202, 885–890.
- Li, L., Barrett, A.D.T., Beasley, D.W.C., 2005. Differential expression of domain III neutralizing epitopes the envelope proteins of West Nile virus strains. *Virology* 325, 99–105.
- Lok, S.M., Ng, M.L., Aaskov, J., 2001. Amino acid and phenotypic changes in dengue 2 virus associated with escape from neutralisation by IgM antibody. *J. Med. Virol.* 65, 315–323.
- Modis, Y., Ogata, S., Clements, D., Harrison, S.C., 2003. A ligand-binding pocket in the dengue virus envelope glycoprotein. *Proc. Natl. Acad. Sci. U.S.A.* 100, 6986–6991.
- Monath, T.P., 1994. Dengue: the risk to developed and developing countries. *Proc. Natl. Acad. Sci. U.S.A.* 91, 2395–2400.
- Nybakk, G.E., Oliphant, T., Johnson, S., Burke, S., Diamond, M.S., Fremont, D.H., 2005. Structural basis of West Nile virus neutralization by a therapeutic antibody. *Nature* 437, 764–769.
- Rodriguez-Roche, R., Alvarez, M., Gritsun, T., Rosario, D., Halstead, S., Kouri, G., Gould, E.A., Guzman, M.G., 2005. Dengue virus type 2 in Cuba, 1997: conservation of E gene sequence in isolates obtained at different times during the epidemic. *Arch. Virol.* 150, 415–425.
- Roehrig, J.T., 2003. Antigenic structure of flavivirus proteins. *Adv. Virus Res.* 59, 141–175.
- Roehrig, J.T., Johnson, A.J., Hunt, A.R., Bolin, R.A., Chu, M.C., 1990. Antibodies to dengue 2 virus E-glycoprotein synthetic peptides identify antigenic conformation. *Virology* 177, 668–675.
- Roehrig, J.T., Bolin, R.A., Kelly, R.G., 1998. Monoclonal antibody mapping of the envelope glycoprotein of the dengue 2 virus, Jamaica. *Virology* 246, 317–328.
- Sabin, A.B., 1952. Research on dengue during World War II. *Am. J. Trop. Med. Hyg.* 1, 30–50.
- Samuel, S., Koh, C.L., Blok, J., Pang, T., Lam, S.K., 1989. Nucleotide sequence of the envelope protein gene of a Malaysian dengue-2 virus isolated from a patient with dengue haemorrhagic fever. *Nucleic Acids Res.* 17, 8875.
- Serafin, I.L., Aaskov, J.G., 2001. Identification of epitopes on the envelope (E) protein of dengue 2 and dengue 3 viruses using monoclonal antibodies. *Arch. Virol.* 146, 2469–2479.
- Shepherd, C.M., Borelli, I.A., Lander, G., Natarajan, P., Siddavanahalli, V., Bajaj, C., Johnson, J.E., Brooks, C.L., Reddy, V.S., 2006. VIPERdb: a relational database for structural virology. *Nucleic Acids Res.* 34, D386–D389.
- Smith, T.J., Olson, N.H., Cheng, R.H., Liu, H., Chase, E.S., Lee, W.M., Leippe, D.M., Mossner, A.G., Rueckert, R.R., Baker, T.S., 1993. Structure of human rhinovirus complexed with Fab fragments from a neutralizing antibody. *J. Virol.* 67, 1148–1158.
- Stewart, P.L., Chiu, C.Y., Huang, S., Muir, T., Zhao, Y., Chait, B., Mathias, P., Nemerow, G.R., 1997. Cryo-EM visualization of an exposed RGD epitope on adenovirus that escapes antibody neutralization. *EMBO J.* 16, 1189–1198.
- Taylor, H.P., Armstrong, S.J., Dimmock, N.J., 1987. Quantitative relationships between an influenza virus and neutralizing antibody. *Virology* 159, 288–298.
- Thullier, P., Demangel, C., Bedouelle, H., Megret, F., Jouan, A., Deubel, V., Mazie, J.C., Lafaye, P., 2001. Mapping of a dengue virus neutralizing epitope critical for the infectivity of all serotypes: insight into the neutralization mechanism. *J. Gen. Virol.* 82, 1885–1892.
- Trirawatanapong, T., Chandran, B., Putnak, R., Padmanabhan, R., 1992. Mapping of a region of dengue virus type-2 glycoprotein required for binding by a neutralizing monoclonal antibody. *Gene* 116, 139–150.
- Wu, K.P., Wu, C.W., Tsao, Y.P., Kuo, T.W., Lou, Y.C., Lin, C.W., Wu, S.C., Cheng, J.W., 2003. Structural basis of a flavivirus recognized by its neutralizing antibody: solution structure of the domain III of the Japanese encephalitis virus envelope protein. *J. Biol. Chem.* 278, 46007–46013.
- Zhang, W., Chipman, P.R., Corver, J., Johnson, P.R., Zhang, Y., Mukhopadhyay, S., Baker, T.S., Strauss, J.H., Rossmann, M.G., Kuhn, R.J., 2003. Visualization of membrane protein domains by cryo-electron microscopy of dengue virus. *Nat. Struct. Biol.* 10, 907–912.